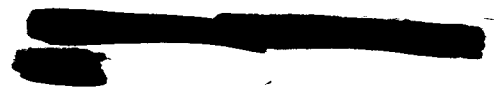


TRANSPORT PROPERTIES OF HIGH TEMPERATURE GASES

by Richard S. Brokaw

Lewis Research Center
Cleveland, Ohio



TECHNICAL PAPER proposed for presentation at
Third International Symposium on High Temperature Technology
sponsored by Stanford Research Institute
Pacific Grove, California
September 17-20, 1967

NATIONAL AERONAUTICS AND SPACE ADMINISTRATION

TRANSPORT PROPERTIES OF HIGH TEMPERATURE GASES

Richard S. Brokaw

Lewis Research Center
National Aeronautics and Space Administration
Cleveland, Ohio

INTRODUCTION

E-4009

The transport properties of dilute monatomic gases at low to moderate temperatures are now well-understood; the rigorous Chapman-Enskog Theory appears to provide an entirely adequate description for these gases. The theory applies to molecules with spherically symmetrical intermolecular force fields and hence is not strictly applicable to polyatomic gases. In practice, however, it turns out that theory gives a good account of the viscosities and diffusion coefficients of polyatomic gases and gas mixtures. The thermal conductivity poses a special problem, however, because internal energy modes - rotation, vibration, etc. - make a contribution to the heat flux. Here there has been recent progress - notably the work of Mason and Monchick^{1, 2} - so that we now have an improved understanding of the problem, sufficient for most practical purposes. For example, if we know the viscosity of a gas and something of its molecular properties (heat capacity, moments of inertia, dipole moment, if any) we should be able to predict its thermal conductivity within a few percent (except, perhaps, for strongly polar gases).

Consequently in this paper I take the position that we have an adequate theoretical framework for predicting transport properties of high temperature gases, and that differences from room temperature gases arise as a consequence of phenomena not usually encountered at modest temperatures - for example, the presence of mobile chemical equilibria, or the presence of atoms or free radicals which are valence unsaturated. As a starting point the next section discusses briefly transport properties of gases at moderate temperatures. That will be followed with a section on heat conduction in chemically reacting gas mixtures, and then a section on the effect of the "unusual" intermolecular forces between labile atoms and/or free radicals. The paper concludes with a discussion of some of the unique phenomena in ionized gases (plasmas).

TM X-52315

TRANSPORT PROPERTIES AT MODERATE TEMPERATURES

The rigorous Chapman-Enskog theory leads to the following expressions for the transport properties of dilute monatomic gases³:

Viscosity

$$\eta = \frac{5}{16} \left(\frac{\sqrt{\pi m k T}}{\pi \sigma^2 \Omega(2, 2)^*} \right) \quad (1)$$

Thermal conductivity

$$\lambda = \frac{25}{32} \left(\frac{\sqrt{\pi m k T}}{\pi \sigma^2 \Omega(2, 2)^*} \right) \left(\frac{c_v}{m} \right) \quad (2)$$

Self-diffusion coefficient

$$D = \frac{3}{8} \left(\frac{\sqrt{\pi m k T}}{\pi \sigma^2 \Omega(1, 1)^*} \right) \frac{1}{\rho} \quad (3)$$

These formulas involve well-known quantities such as the atomic mass m , the Boltzmann constant k , the temperature T , the heat capacity $c_v (= \frac{3}{2} k)$, and the density ρ . In addition the formulas contain cross sections, (or collision integrals) $\sigma^2 \Omega(2, 2)^*$ and $\sigma^2 \Omega(1, 1)^*$ and to compute these the intermolecular force law must be known. However, the potential appears explicitly in an integrand which is then averaged by three integrations. Consequently the collision integrals are not very sensitive to the details of the intermolecular potential.

Figure 1 compares experimental and calculated viscosity data for argon over a wide temperature range. The curve has been computed for the potential energy function shown in the inset in Fig. 1 (a combination of an inverse sixth power attractive potential, which has a theoretical basis in the dispersion forces, with an exponential repulsion). The potential has been chosen⁴ to take account of equation-of-state and crystal properties as well as viscosity coefficients. For example, the interatomic distance in solid argon is 3.8 Å - just inside the minimum of the potential energy curve at 3.866 Å. And the depth of the attractive well - 123.2° K - is consistent with argon's heat of sublimation of 0°K. The same potential successfully describes the thermal conductivity (Fig. 2) and self-diffusion coefficients (Fig. 3) for argon.

For gas mixtures the expressions for the viscosity and thermal conductivity are algebraically complicated and contain cross sections characteristic of interactions between unlike molecules. In principle this requires a knowledge of the intermolecular potential between the unlike species; however, in practice, rough estimates based on empirical combination rules which average potential parameters of the pure components work reasonably well for the valence-saturated gases encountered at ordinary temperatures. With mixtures of polar and nonpolar gases the polar-nonpolar interactions are essentially of a nonpolar nature; hence the unlike cross sections are smaller than might be inferred from a simple averaging of the cross sections of the pure components.

Experimental viscosities of nitrogen-hydrogen⁵ and ammonia-hydrogen⁶ mixtures are shown in figure 4. The solid lines have been computed using empirical combination rules to estimate the $N_2 - H_2$ and $NH_3 - H_2$ intermolecular potentials. The agreement between theory and experiment is generally good (although for $NH_3 - H_2$ mixtures the accord is even better if experimental diffusion coefficients are analyzed to estimate the $NH_3 - H_2$ potential⁷). The dashed curve for $NH_3 - H_2$ mixtures was calculated assuming the $NH_3 - H_2$ cross section to be the geometric mean of the $NH_3 - NH_3$ and $H_2 - H_2$ cross sections. This procedure (which works reasonably well for nonpolar mixtures) overestimates the cross section so that the predicted viscosities are too low.

Experimental thermal conductivities⁸ for these same mixtures are shown in figure 5. The curves, calculated using Hirschfelder's⁹ Eucken-type approximation for gas mixtures, agree reasonably well with experiment, although the errors are larger than in the case of viscosity. This is in part due to larger experimental errors, but may also be due to approximations in the theory. (But a more sophisticated theory for gas mixtures seems scarcely better².)

Thus we have adequate theory for predicting transport properties of dilute gases. The remainder of the paper will be devoted to the phenomena which do not usually arise in room temperature gases.

HEAT CONDUCTION IN CHEMICALLY REACTING GASES

At high temperatures many gases are partially dissociated and undergo a variety of chemical reactions. In reacting gases, heat transport may be considerably larger than in 'frozen' (nonreacting) mixtures. Large amounts of heat can be carried as chemical enthalpy of molecules that diffuse because the gas composition varies with temperature. For example, in a gas that absorbs heat by dissociating as the temperature is raised heat is transported when a molecule dissociates in the high-temperature region and the fragments diffuse toward the cooler region. In the low-temperature region the fragments recombine and release the heat absorbed at high temperature.

When chemical reaction rates are very high, chemical equilibrium can be assumed to exist locally throughout a gas mixture. It is then possible, by differentiating the equilibrium relations, to relate the concentration gradients to the temperature gradient. In this event one can define an equilibrium thermal conductivity λ_e independent of apparatus geometry and scale:

$$\lambda_e = \lambda_f + \lambda_r \quad (4)$$

where λ_f is the conductivity in the absence of reaction (the 'frozen' thermal conductivity) and λ_r is the augmentation due to the reactions.

A general expression for the thermal conductivity due to chemical reactions has been developed^{9, 10} that is applicable to mixtures involving any number of reactants, inert diluents, and chemical equilibria, provided chemical equilibrium exists locally in the temperature gradient. For a simple dissociation of the type $A \rightleftharpoons nB$ the thermal conductivity due to chemical reaction is

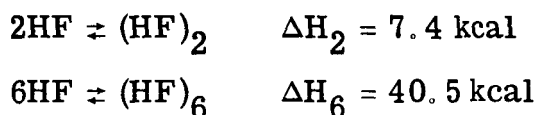
$$\lambda_r = \frac{D_{AB} P}{RT} \frac{\Delta H^2}{RT^2} \frac{x_A x_B}{(nx_A + x_B)^2} \quad (5)$$

Here D_{AB} is the binary diffusion coefficient between components A and B, ΔH is the heat of reaction, and x_A , x_B are the mole fractions of the components. Note that unless both species are present, λ_r is zero. Furthermore, since in a dissociating gas the composition varies with pressure, we expect the heat conductivity to vary with pressure also. This is in con-

trast to the behavior of nonreacting gases, for which the heat conductivity is independent of pressure.

Experimental¹¹ and theoretical¹² conductivities for the $\text{N}_2\text{O}_4 \rightleftharpoons 2\text{NO}_2$ system at one atmosphere are shown in figure 6. The dashed curve indicates the frozen conductivity. Thus λ_r is the major contribution to the heat conductivity; at the maximum (where the mass fractions of N_2O_4 and NO_2 are equal) the conductivity is comparable to that of a light gas such as helium, and an order of magnitude greater than in the chemically frozen gas mixture.

The theoretical expression for a system involving two reactions has been tested¹³ for the case of hydrogen fluoride vapor. At moderate pressures the PVT behavior of hydrogen fluoride can be described in terms of a monomer-hexamer equilibrium, while low pressure data suggest a dimer as well. Although the actual state of the vapor is uncertain, it appears that at low and moderate pressures the equilibria



serve to specify the system rather well.

Computed and experimental¹⁴ thermal conductivities are compared in Fig. 7. The solid line was computed assuming both dimer and hexamer equilibria, whereas the dashed line was computed considering only the hexamer equilibrium. Note the extreme pressure dependence of the thermal conductivity. The maximum conductivity is more than three times that of hydrogen at the same temperature and some 33 times the frozen thermal conductivity expected in the absence of reaction. The inclusion of a dimer equilibrium markedly improves the agreement between theory and experiment in the low-pressure region.

The experimental studies on nitrogen tetroxide and hydrogen fluoride prove the validity of the theoretical expressions for thermal conductivity of reacting gases in chemical equilibrium. The theory has also been successfully applied to data for the $\text{PCl}_5 \rightleftharpoons \text{PCl}_3 + \text{Cl}_2$ equilibrium¹⁵.

Thus far we have considered systems where the chemical reactions

are so rapid that chemical equilibrium prevails locally at all points in the gas mixture. Let us now consider the reduction of heat transport caused by reduced reaction rates. A general expression has been derived¹⁶ for the apparent thermal conductivity of reacting mixtures in which a single reaction proceeds at a finite rate. In contrast to systems where reaction rates are either very high or very low, it is found that heat conduction depends on the geometry and scale of the system and also the catalytic activity of the surfaces.

For a plane parallel plate geometry, with one surface noncatalytic and the other surface a perfect catalyst, the effective thermal conductivity is

$$\lambda^* = \frac{\lambda_e \lambda_f}{\lambda_f + \lambda_r \left[\frac{\tanh \varphi}{\varphi} \right]} \quad (6)$$

where

$$\varphi^2 \equiv \frac{\lambda_e}{\lambda_f \lambda_r} \frac{\Delta H^2}{RT^2} \mathcal{R} \ell^2$$

Here \mathcal{R} is the chemical reaction rate at equilibrium (that is the total rate in either direction - not the net rate, which is zero, of course), and ℓ is the distance between the plates. For simple systems it can be shown that

$$\varphi^2 = \frac{\lambda_e}{\lambda_f} \frac{\tau_{\text{Diff}}}{\tau_{\text{Chem}}} \quad (7)$$

If the diffusion time τ_{Diff} is short in comparison with the chemical relaxation time τ_{Chem} , $\varphi \rightarrow 0$, $\tanh \varphi / \varphi \rightarrow 1$, and $\lambda^* \rightarrow \lambda_f$. In other words, the concentration gradients are washed out by diffusion and the frozen conductivity is obtained. On the other hand if the chemical time is short, the concentration gradients are maintained, $\varphi \rightarrow \infty$, $\tanh \varphi / \varphi \rightarrow 0$, and $\lambda^* \rightarrow \lambda_e$.

The theory can be applied to low-pressure measurements¹¹ on the $\text{N}_2\text{O}_4 \rightleftharpoons 2\text{NO}_2$ system, as shown in figure 8. The upper and lower dashed curves are respectively, the computed equilibrium and frozen conductivities.

The solid curve has been fitted to the data assuming negligible surface reaction and assuming that the rate constant for the dissociation reaction



is $5.3 \times 10^9 \text{ cm}^3 \text{ mole}^{-1} \text{ sec}^{-1}$ at 296° K . This is in reasonable agreement values derived from ultrasonic absorption measurements by Sessler¹⁷ (4.7×10^9) and by Cher¹⁸ (4.1×10^9).

Thus we seem to have an adequate understanding of the effects of chemical reaction on heat conduction. This is fortunate, because these mobile chemical equilibria are frequently encountered in high temperature gas mixtures.

MULTIPLE INTERACTION CURVES AND THE PROPERTIES OF LABILE ATOMS AND FREE RADICALS

The discussion thus far has been concerned with systems in which it is assumed that a pair of colliding atoms or molecules can interact along only one potential energy curve. However, in collisions between atoms or free radicals possessing unpaired electron spins multiple interaction curves are possible. For example if two hydrogen atoms collide with spins opposed they follow the $^1\Sigma$ attractive potential (which corresponds to the H_2 molecule); this occurs on one collision in four. On the otherhand in three out of four collisions the spins are parallel and the atoms follow the antibonding $^3\Sigma$ repulsive potential. With other atoms these interactions can be much more complex - two ground state oxygen atoms can follow any of eighteen different potential energy curves¹⁹. It has been shown²⁰ that when there are multiple interaction curves the transport property formulas of classical kinetic theory remain valid, but the collision integrals must be averaged over the different curves, with each one weighted according to its statistical weight.

These interactions between labile atoms or free radicals are usually much stronger than the interactions between valence saturated species, and this in turn has an effect on the transport properties. This is illustrated in Fig. 9 where the viscosities of atomic and molecular hydrogen are compared. The experimental viscosities for hydrogen atoms have been deduced by Browning and Fox²¹ from their measurements on hydrogen atom-molecule mixtures,

assuming an appropriate fit to Margenau's calculation²² of the H - H₂ interaction. The experimental atom viscosities are in near-perfect agreement with the accurate quantal calculations of Buckingham, Browning, and Gal²³, shown as a solid line.

On the otherhand, if one were to naively overlook the ¹Σ and ³Σ potentials and assume weak forces analogous to the H₂ - H₂ and H - H₂ interactions a considerably smaller H atom cross section would be predicted. The dashed curve in figure 9 shows such a prediction based on Lennard-Jones (12-6) potential force constants of $\sigma_{\text{H-H}} = 2.53 \text{ \AA}$, $(\epsilon/k)_{\text{H-H}} = 31.3^\circ \text{ K}$. (There values were obtained from the force constants $\sigma_{\text{H-H}_2} = 2.75 \text{ \AA}$, $(\epsilon/k)_{\text{H-H}_2} = 32.27^\circ \text{ K}^{24}$ and $\sigma_{\text{H}_2\text{-H}_2} = 2.968 \text{ \AA}$, $(\epsilon/k)_{\text{H}_2\text{-H}_2} = 33.3^\circ \text{ K}^{25}$ by inverting the usual combining rules for the potential parameters²⁶.)

Thus the effects due to multiple interaction curves seem well-understood and we find a satisfying agreement between theory and experiment in the case of atomic hydrogen. Of course in high temperature gas mixtures involving many different atoms and radicals the situation may be complex indeed, and it might be necessary to consider hundreds of interactions for a truly rigorous calculation of transport properties. (A reasonably complete treatment for the nitrogen-oxygen system, for high temperature air, includes more than thirty interactions²⁷.) The potential curves for many interactions are known only poorly, if at all - especially some of the repulsive interactions. And the repulsive interactions play an important role because of the high multiplicities which are frequently associated with such states.

TRANSPORT PROPERTIES OF IONIZED GASES

At temperatures in the neighborhood of 10 000^oK and moderate pressures almost all gases are to some extent ionized. Such gases possess unusual properties because of the presence of the very light electrons and because of the very long range Coulomb interaction between the charged species.

The precise experimental determination of the transport properties of plasmas is extremely difficult; hence the usual interplay between theory and accurate experimentation is lacking. Consequently the theory must be developed with sophistication and care.

For unionized gases the lowest non-zero Chapman-Enskog approximation provides a generally adequate description of the transport properties (with the possible exception of the coefficients of thermal diffusion). Consequently some have applied these lowest approximations to ionized gases, although calculations²⁸ for the Lorentzian gas should have suggested the possibility of slow convergence in the case of plasmas. Ahtye²⁹ realized that higher approximations were required and the matter has been further and extensively explored by DeVoto^{30, 31}.

Some of DeVoto's³¹ results for argon at atmospheric pressure are presented in Fig. 10, which shows the ratios of the lowest non-zero Chapman-Enskog approximations to the highest approximations calculated by DeVoto. The ratios are plotted against temperature, with a secondary scale showing the degree of ionization α . The ratio of the first to second approximation for viscosity, $[\eta]_1/[\eta]_2$, is within one percent of unity at low temperatures and drops off to about 0.89 as the gas approaches complete ionization. This is about the same as the ratio DeVoto calculated³⁰ for a fully ionized hydrogen plasma (0.883) and indicates that the first approximation is not sufficient for accurate calculations at high degrees of ionization. The accuracy of the second approximation is not known, but it is probably within one or two percent, if the result for the Lorentzian gas is any guide²⁸.

The ratio of the second to fourth approximation for the translational thermal conductivity, $[\lambda]_2/[\lambda]_4$, (the first Chapman-Enskog approximation is zero) drops to about 0.43 at high temperature, showing that $[\lambda]_2$ is seriously in error ($[\lambda]_2/[\lambda]_4$ for fully ionized hydrogen is 0.438³⁰). DeVoto finds $[\lambda]_3/[\lambda]_4$ within 3 percent of unity, so that $[\lambda]_4$ must be accurate indeed.

The ratio $[\sigma]_1/[\sigma]_4$ indicates that the first approximation to the electrical conductivity is inadequate under any circumstances. At high temperatures the higher approximations converge rapidly - at 10 000^o K the second approximation is within 5 percent of the fourth - but at low temperatures even the fourth approximation seems not to have converged on the true value. For example at 4000^o K, $[\sigma]_2/[\sigma]_4 = 0.63$ and $[\sigma]_3/[\sigma]_4 = 0.82$.

Thus it seems that accurate calculations for ionized gases require the

higher Chapman-Enskog approximations, which are algebraically complicated. It would be very desirable to develop simpler expressions; deVoto³¹ has done some work in this direction.

A partially ionized gas contains at least three species - ions, electrons, and the parent atoms. In order to describe the transport properties cross sections for all the pair-wise interactions must be obtained. Let us consider argon as an example. The interactions are Ar - Ar, Ar - e, Ar - Ar⁺, Ar⁺ - Ar⁺, e - e, and Ar⁺ - e.

If we regard the argon-argon cross section as 'normal', all the other cross sections are in one way or another abnormal or peculiar. Argon atoms are very transparent to electrons so the atom-electron cross section is unusually small (about 0.5 to perhaps 7 Å² compared to 13 - 15 Å for the Ar-Ar cross section³²). On the otherhand the argon atom-ion cross sections appear unusually large. One might at first assume that the atom-ion cross section would be comparable to the atom-atom cross section. However, when an ion encounters its parent atom resonant charge transfer occurs; this gives rise to an exchange force which increases the elastic collision cross sections (by about 80 percent in the case of argon³²). But charge exchange has a further effect on the diffusion or mobility of ions. This resonant exchange is probable on grazing collisions between ions and their parent atoms, and a grazing collision with charge transfer is equivalent to a head-on collision without charge transfer insofar as the transport of charge is concerned.

To a good approximation the contribution of the ionization equilibrium to the heat conductivity is^{9, 33}

$$\lambda_r \cong \frac{D_{\text{Ar-Ar}^+} P}{RT} \frac{\Delta H^2}{RT^2} \frac{x_{\text{Ar}} x_{\text{Ar}^+}}{(x_{\text{Ar}^+} + x_{\text{Ar}^+})^2} \quad (8)$$

Here ΔH is now the heat of ionization while x_{Ar} , x_{Ar^+} are the mole fractions of atoms and ions; the atom-ion diffusion coefficient $D_{\text{Ar-Ar}^+}$ is small because of the large charge transfer cross section.

The consequences of the small atom-electron cross section and large atom-ion cross section are apparent in Fig. 11, where the thermal conductivity of argon at atmospheric pressure is plotted as a function of temper-

ature. An auxiliary scale shows the degree of ionization, α . The curves for the equilibrium and translational heat conductivity were computed by DeVoto³¹ while the curve for atomic argon was calculated by Amdur and Mason³⁴. The experimental data below 5000^o K (filled symbols) are derived from shock tube heat transfer studies^{35, 36}, while the data in the 8000 - 12 000^o K range (open symbols) were deduced from arc temperature profiles³⁷.

Note that the heat conductivity in slightly ionized argon is considerably larger than in the unionized gas. For example at 9300^o K where the gas is only 1 percent ionized the heat conductivity is about 80 percent higher than in atomic argon. This is in part due to the small electron mass, and in part due to the small argon-electron cross section.

Note too that at higher temperatures the ionization reaction contributes to the heat conductivity - for example at 13 500^o K the equilibrium conductivity, λ_e , is about 75 percent larger than the translational conductivity, λ_{trans} . However, this is a rather small increase, in comparison with the eight-to tenfold increase in heat conductivity caused by the dissociation of diatomic molecules⁹. The reason, of course, is the very small ion-atom diffusion coefficient which is in turn a consequence of the large resonant charge transfer cross section.

The ion-ion, electron-electron, and ion-electron interactions are all coulombic, an extremely strong and long range interaction, which makes these cross sections very large; in fact if the collision integrals are evaluated for the simple coulomb potential they are found to diverge³⁸. This difficult is most easily circumvented by cutting off the integration for the cross section at some large distance such as the mean interparticle distance, or better yet, at the Debye length

$$d = \left(\frac{kT}{8\pi n_e e^2} \right)^{1/2} \quad (9)$$

(n_e is the number density of electrons and e is the electronic charge). This procedure is justified by the argument that the electrical charge of

distant particles is effectively screened or neutralized by nearby particles of opposite charge¹.

However, it seems preferable to introduce the assumption of screening at the outset and describe the charged particle interactions by the screened coulomb potential,

$$\varphi_{ij} = \pm \frac{e^2}{r} \exp(-r/d). \quad (10)$$

(The plus sign applies for ion-ion and electron-electron interactions, and the minus sign applies for the ion-electron interaction.) Liboff³⁹ has developed analytic expressions for the collision integrals for this potential which are valid at high temperatures, and recently Mason, Munn, and Smith⁴⁰ have done the necessary numerical work to evaluate the integrals for low temperatures as well.

Normally intermolecular potentials depend on intermolecular distance, and, in the case of polyatomic molecules, on the angular orientation of the molecules. The screened coulomb potential is unique, however, in that the potential itself depends on both temperature and pressure, since the Debye length d is a function of temperature and the charged particle density.

This leads to pressure-dependent cross sections, which is also unique. For example, Liboff's expression for the cross section which is important in determining viscosity is

$$\sigma_{\Omega}^{2,2*} = \left(\frac{e^2}{kT}\right)^2 \left[\frac{3}{4} \ln(kT/e^2) - \frac{1}{4} \ln(8\pi n_e) + \ln 2 - \gamma \right] \quad (11)$$

($\gamma = 0.577 =$ Euler's constant); the other cross sections are similar, but with different numerical constants. When the degree of ionization is small,

¹Following Ahtye and DeVoto, Eq. (9) considers both electrons and ions effective in screening; if electrons only are considered, then $d = (kT/4\pi n_e e^2)^{1/2}$. It would seem reasonable to include screening by the ions in calculating a property such as viscosity, which is determined largely by the heavy ions. On the otherhand, for the heat conductivity, determined mostly by the rapid motions of the electrons, the slow-moving ions probably do not screen effectively. (Private communication from Dr. F. A. Lyman.)

n_e is proportional to the square root of the pressure, whereas in the fully ionized gas n_e varies directly with the pressure. In either case, the cross sections increase as the pressure is lowered so that the viscosity and translational thermal conductivity should increase with increasing pressure.

This effect is shown in Fig. 12, where the viscosity of argon is plotted as a function of temperature for a number of pressures. Most of the calculations are due to Ahtye²⁹ (solid curves); his results at atmospheric pressure agree reasonably closely with DeVoto's³¹ computations (dashed curve). Two features are noteworthy. First of all, at high temperatures the viscosity is pressure dependent, due to the dependence of the shielded coulomb cross sections on electron density. Second, the high temperature viscosities are low, a consequence of the enormous size of the shielded coulomb cross sections.

Two concluding observations about the transport properties of ionized gases are in order. First, what about quantum effects? Mason, Munn and Smith⁴⁰ have considered this question and conclude that quantum corrections are important in high density plasmas (say, $n_e > 10^{20} \text{ cm}^{-3}$) at all temperatures; above $10^6 \text{ }^\circ\text{K}$ quantum effects are important in low density plasmas too. Finally, Mason and Sherman⁴¹ have made estimates of cross sections for symmetric resonant charge exchange between ions differing by one in electronic charge - processes such as $\text{Ar}^+ + \text{Ar}^{++} \rightarrow \text{Ar}^{++} + \text{Ar}^+$. They find that at most temperatures and electron densities of interest these cross sections are negligible in comparison to the screened coulomb cross sections for diffusion. This means that resonant charge transfer between ions will not affect the thermal conductivity of plasmas by depressing the rate of diffusive transport of ionization energy. This is in contrast to the situation in partially ionized gases, where, as we have already seen, ion-neutral exchange is important. Thus it appears that theory is adequate for calculating properties of multiply ionized plasmas, provided only that quantum effects are negligible, and the shielded coulomb potential is appropriate for describing interactions between charged particles $[T^3/n_e > 10^{-7} (\text{ }^\circ\text{K}/\text{cm})^3]$.

CONCLUDING REMARKS

I hope the foregoing sections convince the reader that we do indeed have

the theoretical tools for estimating high temperature transport properties. We must be certain that we consider all important aspects - effects due to chemical reactions, multiple interaction curves, and, in partially ionized gases, charge transfer and the long range coulomb forces. In ionized gases we must also take account of the higher Chapman-Enskog approximations, and in this regard algebraic simplifications would be most welcome. Then too, for many interactions between valence unsaturated atoms or free radicals the multiple intermolecular potentials are unknown. But this is a problem of quantum chemistry, and not a concern of transport theory per se.

REFERENCES

1. E. A. Mason and L. Monchick, *J. Chem. Phys.* 36, 1622 (1962).
2. L. Monchick, A. N. G. Pereira, and E. A. Mason, *J. Chem Phys.* 42, 3241 (1965).
3. J. O. Hirschfelder, C. F. Curtiss, and R. B. Bird, Molecular Theory of Gases and Liquids, Wiley, New York, 1954, p. 527.
4. E. A. Mason and W. E. Rice, *J. Chem. Phys.* 22, 843 (1954).
5. M. Trautz and P. B. Baumann, *Ann. Physik* 5, 733 (1929).
6. M. Trautz and R. Heberling, *Ann. Physik* 10, 155 (1931).
7. R. S. Brokaw, R. A. Svehla, and C. E. Baker, NASA Tech. Note TN D-2580, January 1965.
8. P. Gray and P. G. Wright, *Proc. Roy. Soc. (London)* A263, 161 (1961).
9. J. N. Butler and R. S. Brokaw, *J. Chem. Phys.* 26, 1636 (1957).
10. R. S. Brokaw, *J. Chem. Phys.* 32, 1005 (1960).
11. K. P. Coffin and D. O'Neal, Jr., NACA Tech. Note 4209, February 1958.
12. R. S. Brokaw and R. A. Svehla, *J. Chem. Phys.* 44, 4643 (1966).
13. R. S. Brokaw, *Planet. Space Sci.* 3, 238 (1961).
14. E. U. Franck and W. Spalthoff, *Naturwissenschaften* 40, 580 (1953).
15. P. K. Chakraborti, *J. Chem. Phys.* 38, 575 (1963).
16. R. S. Brokaw, *J. Chem. Phys.* 35, 1569 (1961).
17. G. Sessler, *Acustica* 10, 44 (1960).
18. M. Cher, *J. Chem. Phys.* 37, 2564 (1962).

19. J. T. Vanderslice, E. A. Mason, and W. G. Maisch, *J. Chem. Phys.* 32, 515 (1960).
20. E. A. Mason, J. T. Vanderslice, and J. M. Yos, *Phys. Fluids* 2, 688 (1959).
21. R. Browning and J. W. Fox, *Proc. Roy. Soc. (London)* A278, 274 (1964).
22. H. Margenau, *Phys. Rev.* 66, 303 (1944).
23. R. A. Buckingham, R. Browning, and E. Gal, *Proc. Roy. Soc. (London)* A284, 237 (1965).
24. D. G. Clifton, *J. Chem. Phys.* 35, 1417 (1961).
25. Reference 3, p. 1110.
26. Reference 3, Eqs. 8.4-8 and 8.4-9, p. 567.
27. K. S. Yun and E. A. Mason, *Phys. Fluids* 5, 380 (1962).
28. S. Chapman and T. G. Cowling, *The Mathematical Theory of Non-Uniform Gases*, Cambridge University Press, 1958, pp. 193-198.
29. W. F. Ahtye, NASA Tech. Note D-2611, January 1965.
30. R. S. deVoto, *Phys. Fluids* 9, 1230 (1966).
31. R. S. deVoto, *Phys. Fluids* 10, 354 (1967).
32. R. S. deVoto, Stanford University, Dept. of Aeronautics and Astronautics Rept. SUDAER No. 217, February 1965.
33. W. E. Meador, Jr., and L. D. Staton, *Phys. Fluids* 8, 1694 (1965).
34. I. Amdur and E. A. Mason, *Phys. Fluids* 1, 370 (1958).
35. E. F. Smiley, PhD Dissertation, Catholic University of America Press, 1957.
36. D. J. Collins and W. A. Menard, *J. Heat Transfer* 88, 52 (1966).
37. C. F. Knopp and A. B. Cambel, *Phys. Fluids* 9, 989 (1966).
38. Reference 28, pp. 177-179.
39. R. L. Liboff, *Phys. Fluids* 2, 40 (1959).
40. E. A. Mason, R. J. Munn, and F. J. Smith, University of Maryland Rept. IMP-NASA-60, March 31, 1967.
41. E. A. Mason and M. P. Sherman, *Phys. Fluids* 9, 1989 (1966).

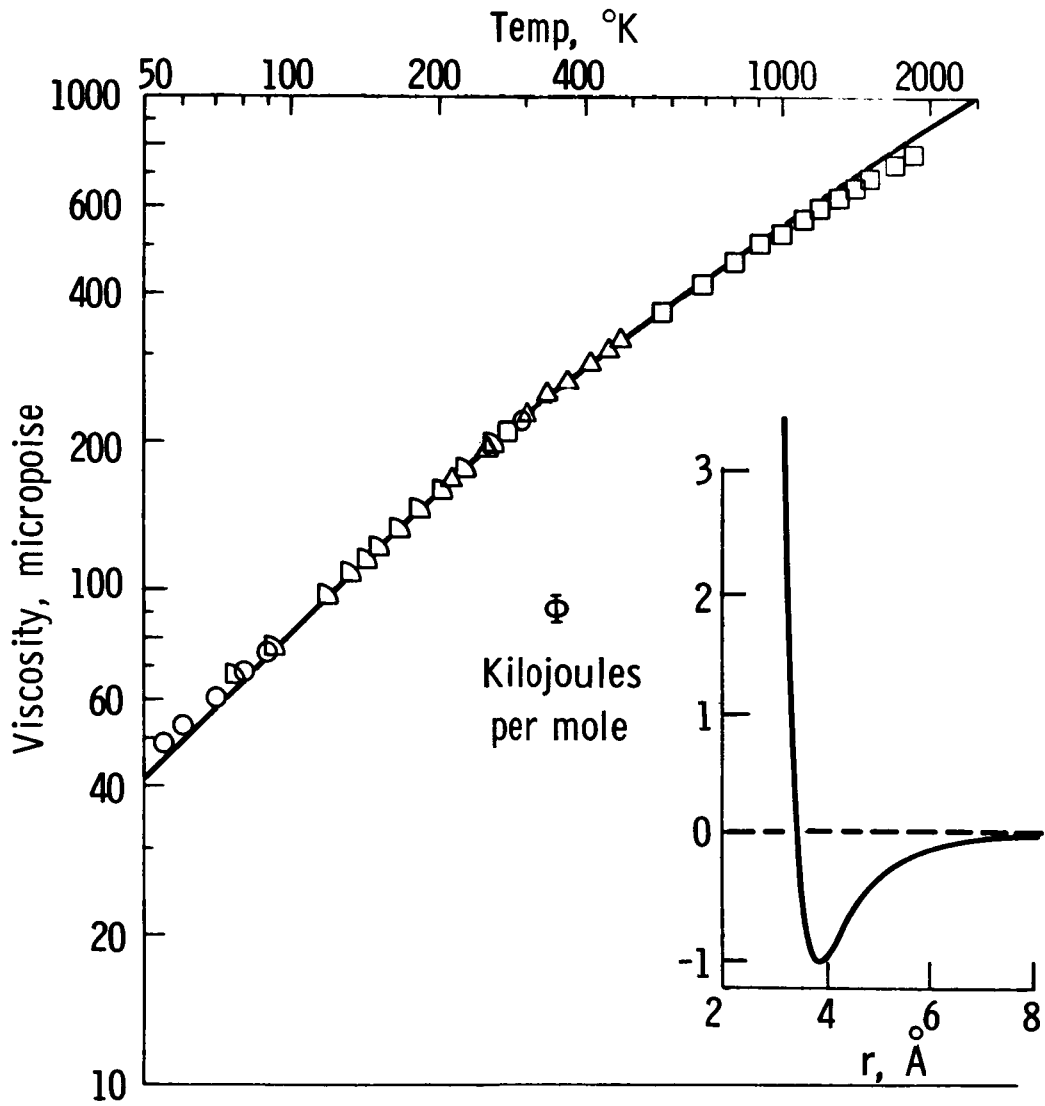


Fig. 1. - Viscosity of argon. Comparison of theory and experiment.

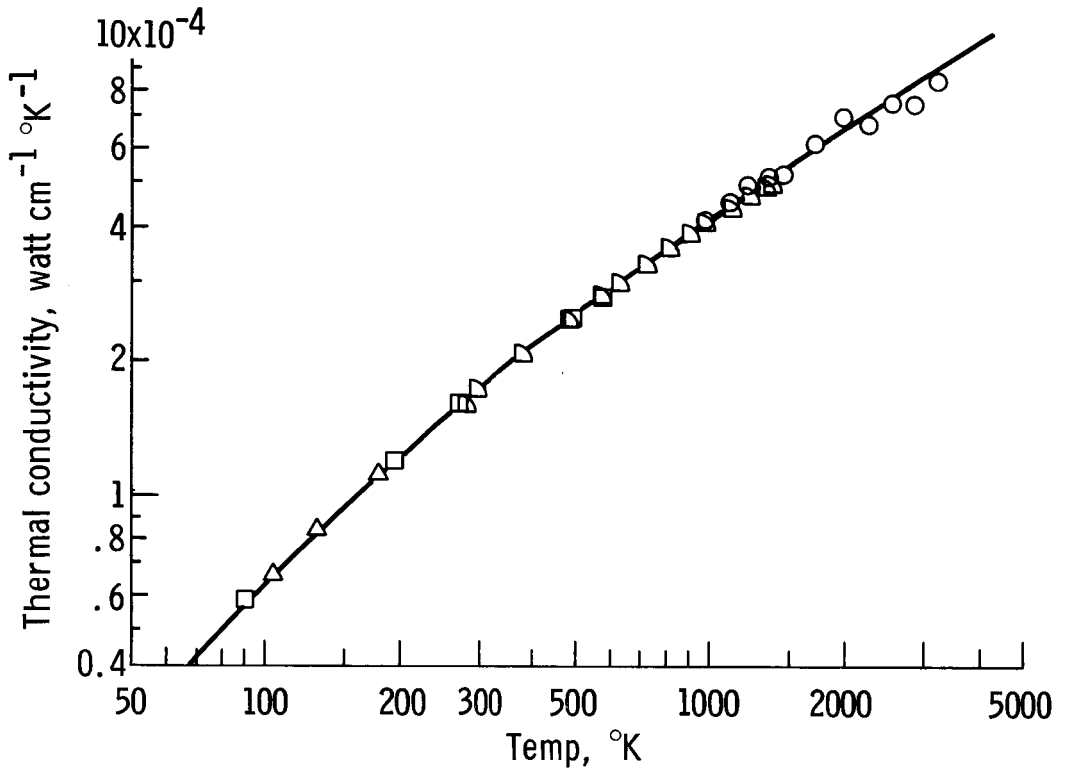


Fig. 2. - Thermal conductivity of argon. Comparison of theory and experiment.

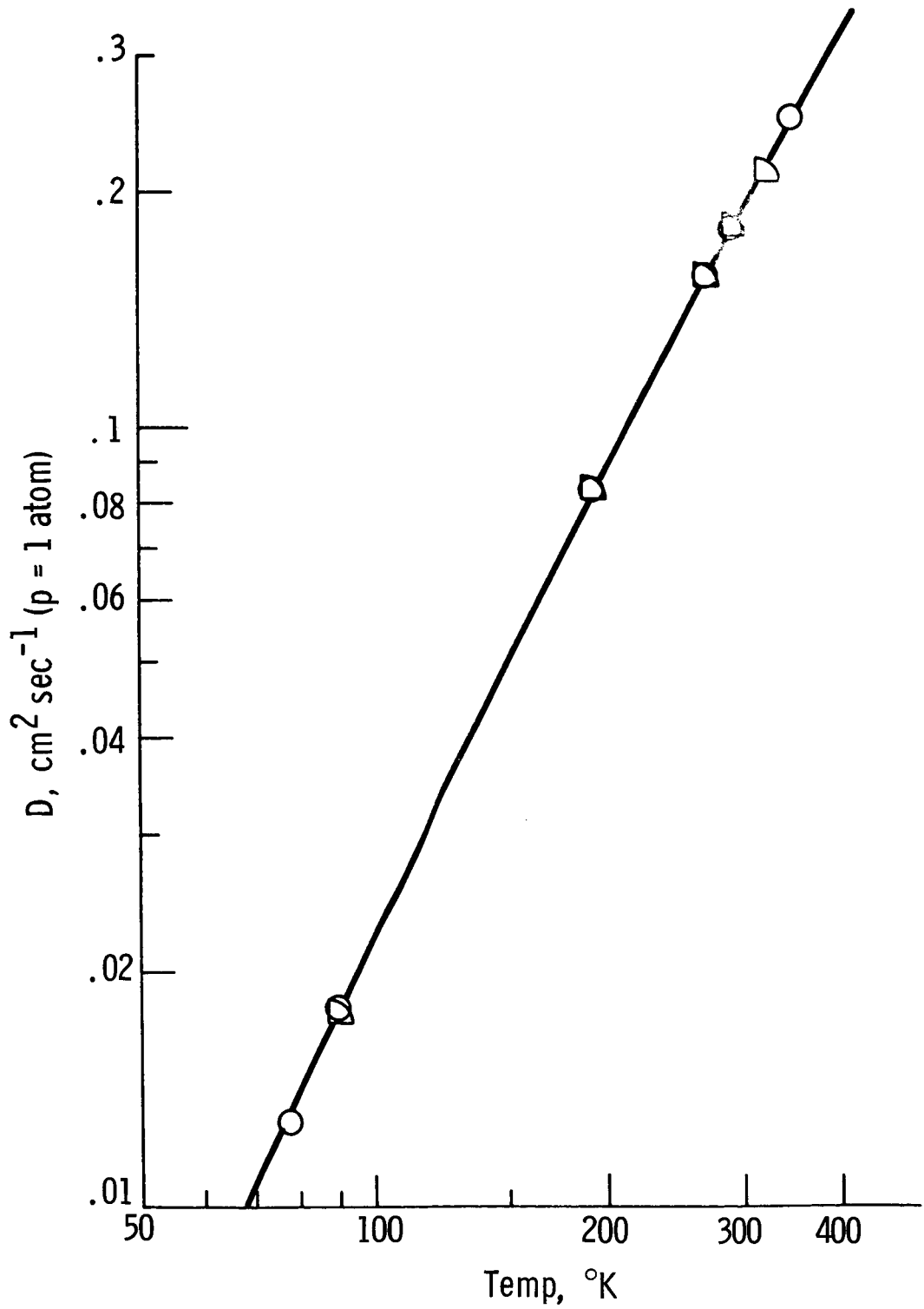


Fig. 3. - Self-diffusion coefficient of argon.
Comparison of theory and experiment.

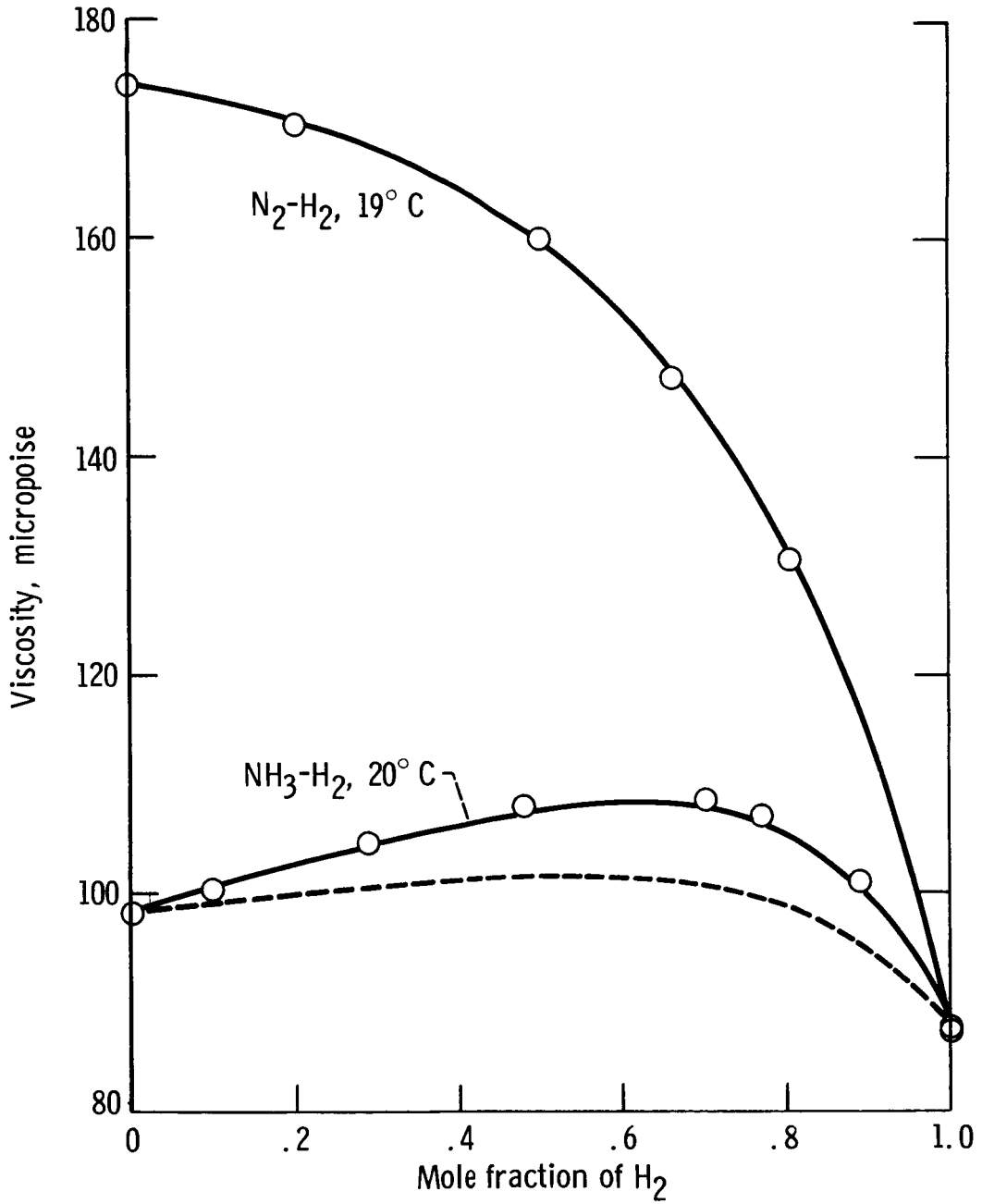


Fig. 4. - Viscosity of gas mixtures. Comparison of theory and experiment.

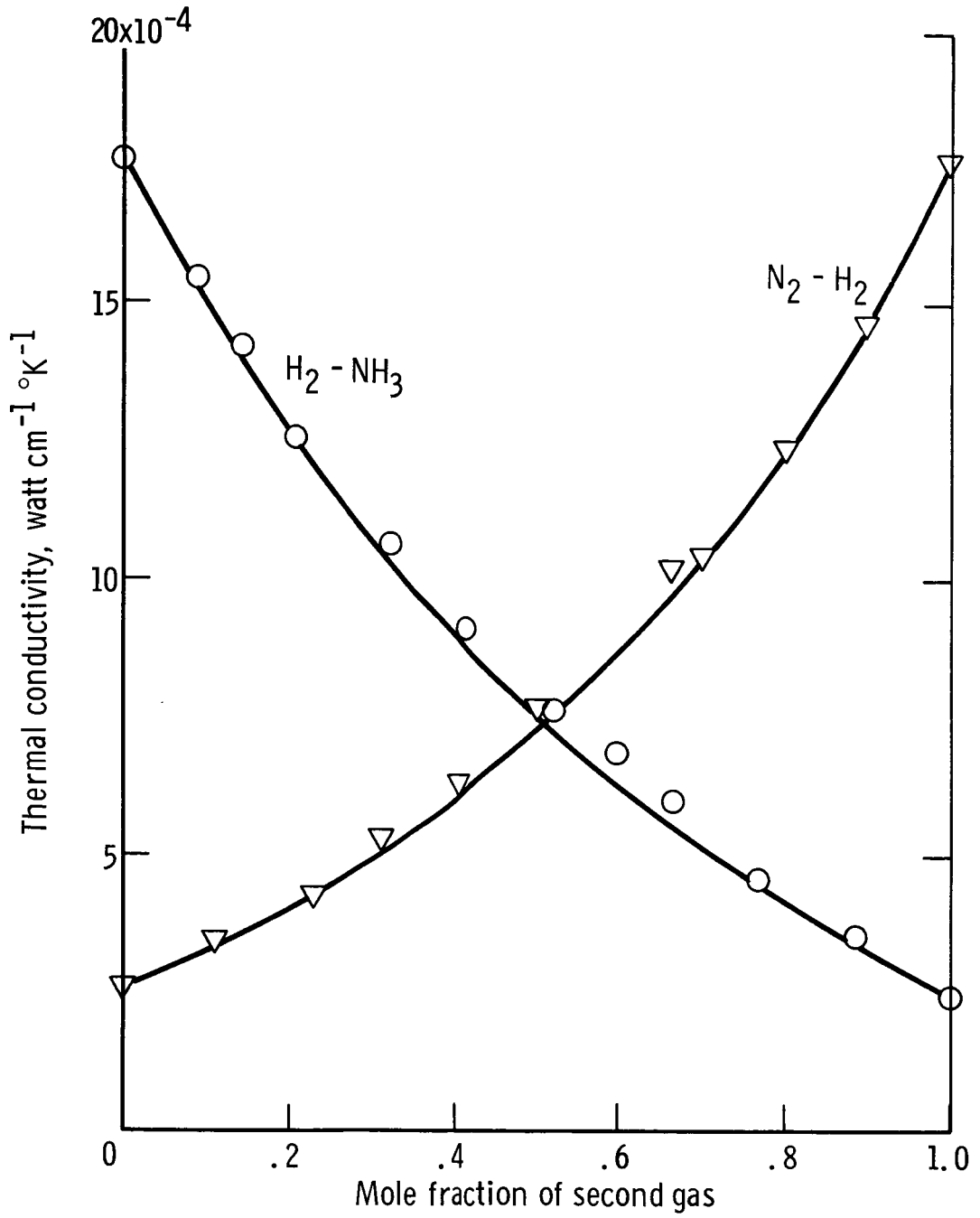


Fig. 5. - Thermal conductivity of gas mixtures, 253° C. Comparison of theory and experiment.

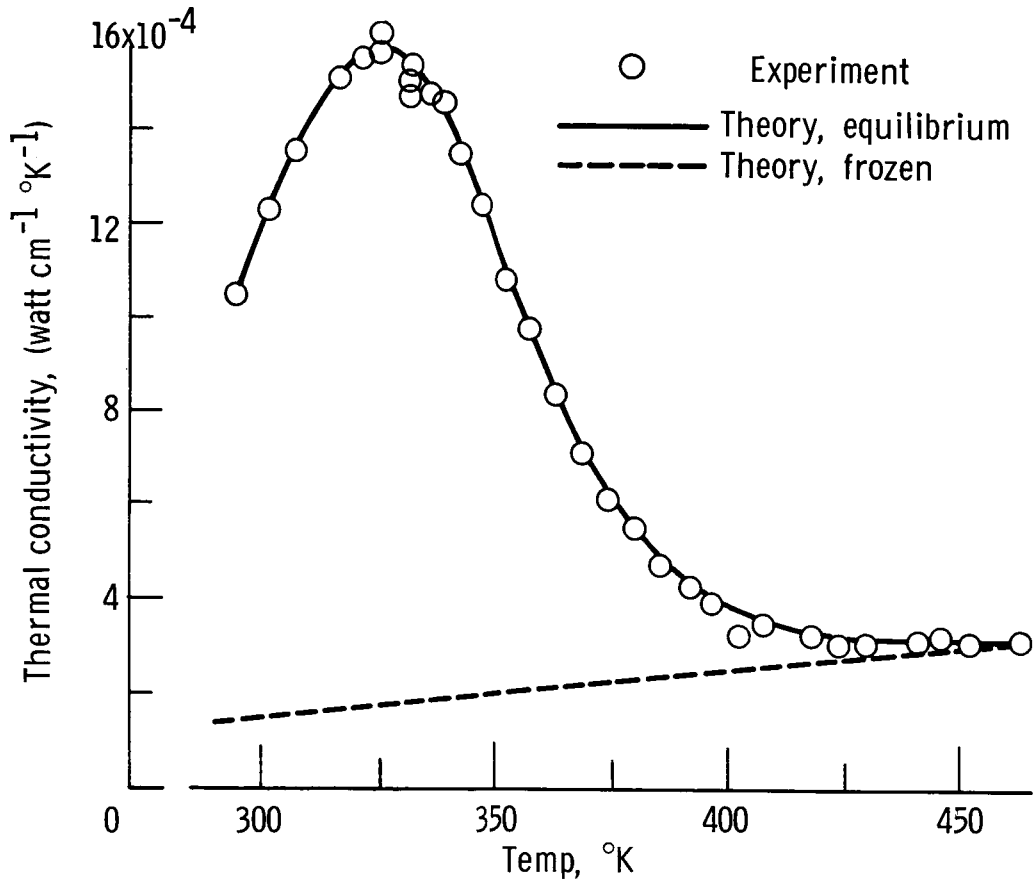


Fig. 6. - Thermal conductivity of nitrogen tetroxide - nitrogen dioxide system. $P = 1$ atm. (ref. 12).

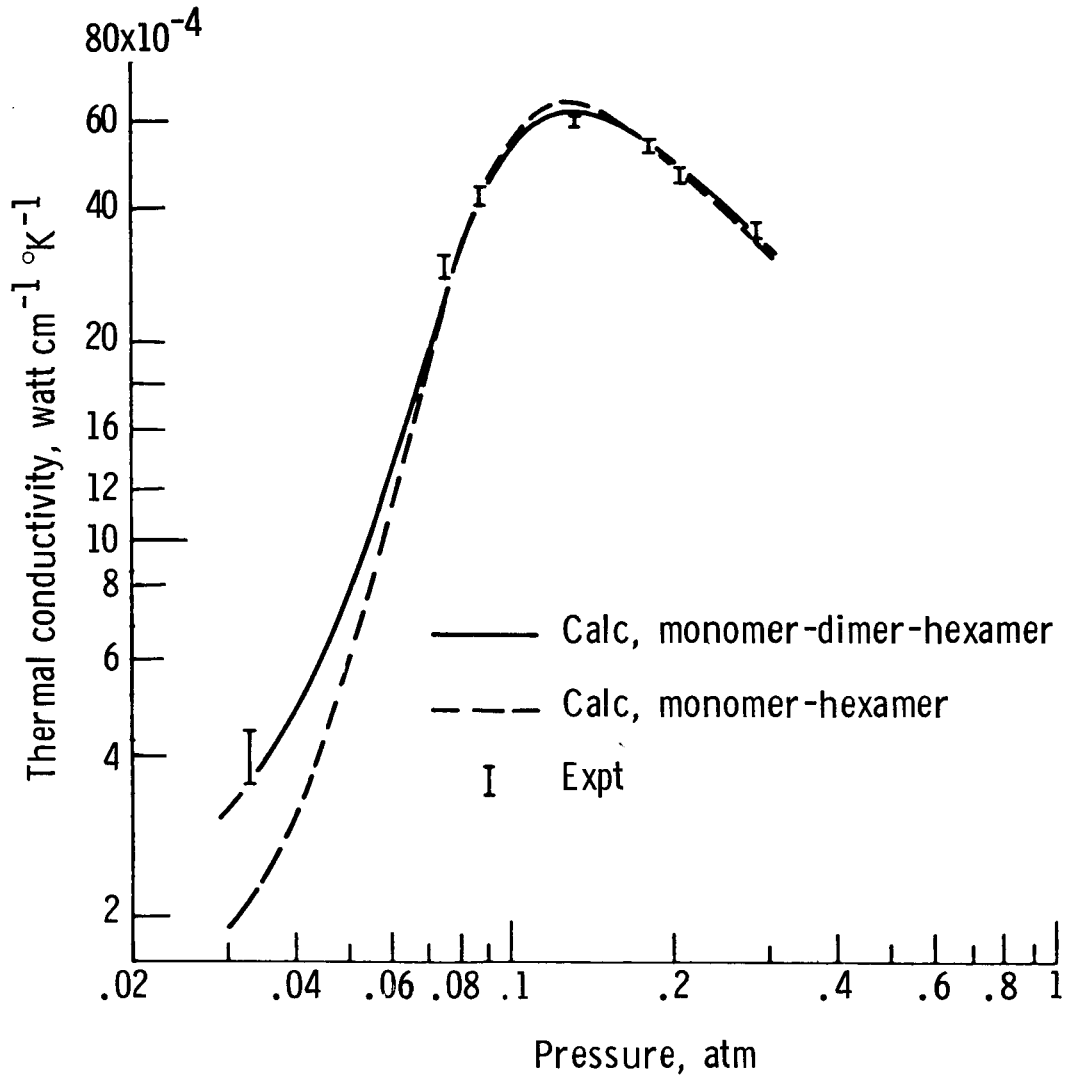


Fig. 7. - Thermal conductivity of hydrogen fluoride vapor at 267.7°K .

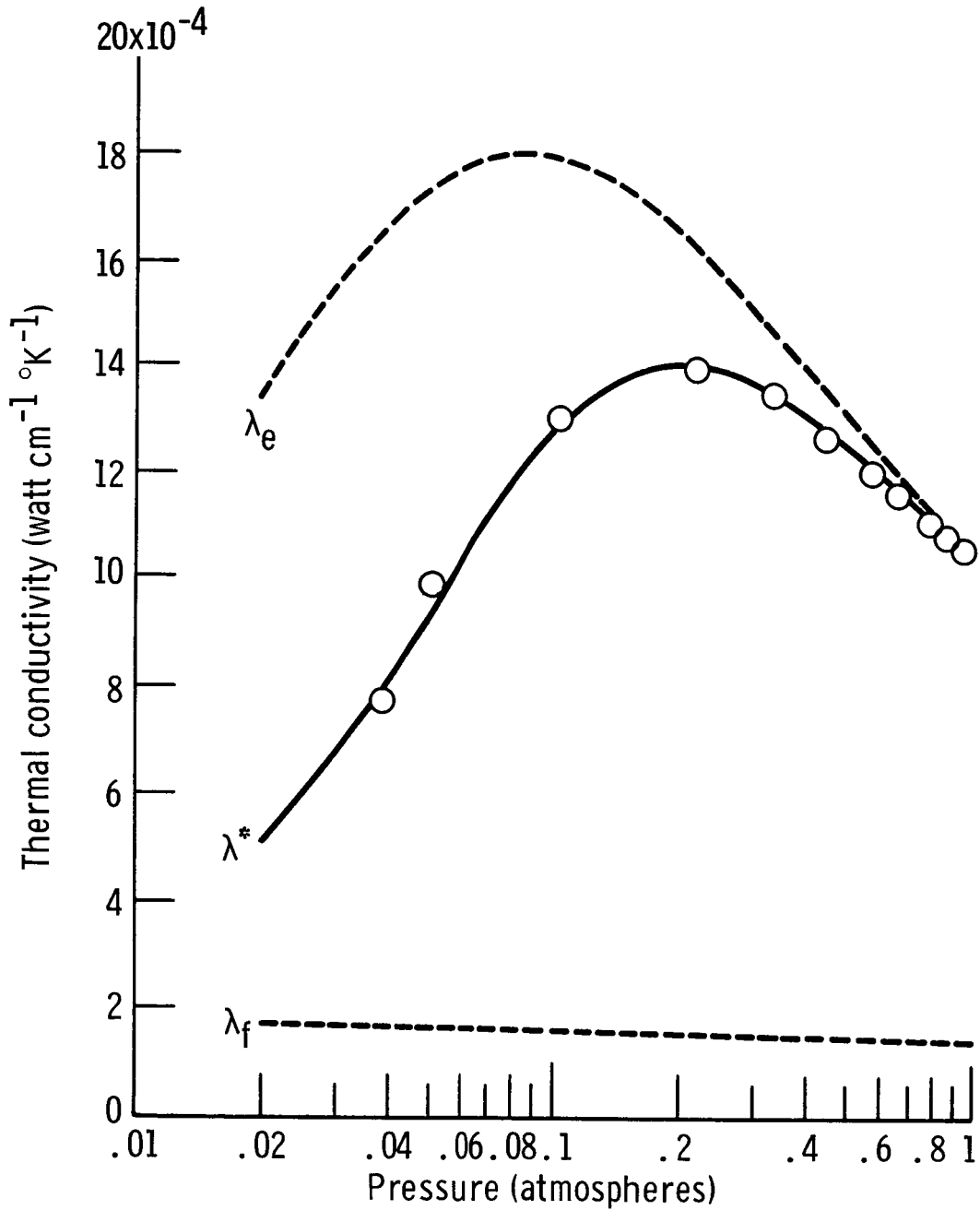


Fig. 8. - Effect of chemical reaction rate on thermal conductivity of $\text{N}_2\text{O}_4 \rightleftharpoons 2\text{NO}_2$ system. $T = 296^\circ \text{K}$. (Ref. 16).

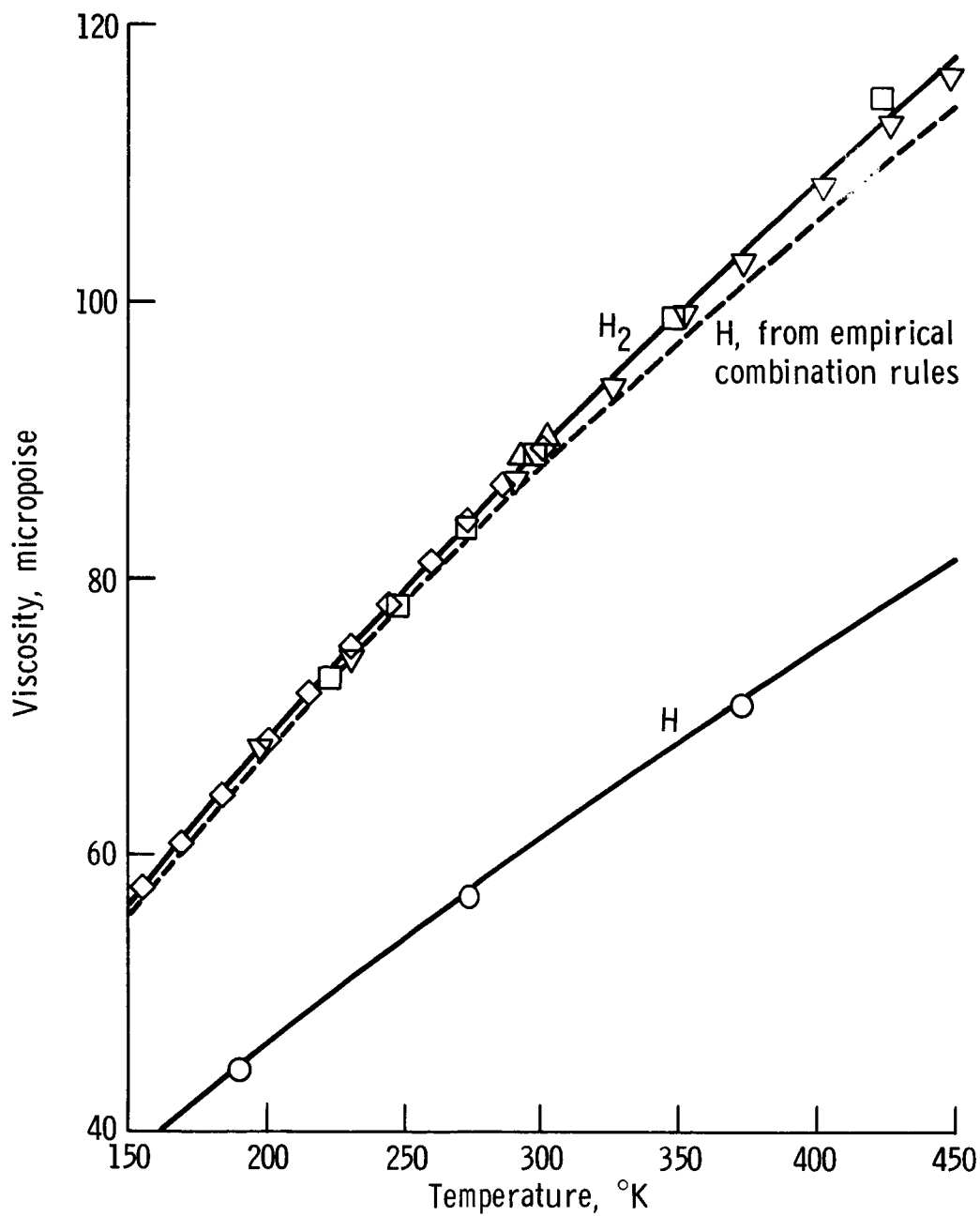


Fig. 9. - Viscosities of atomic and molecular hydrogen.

E-4009

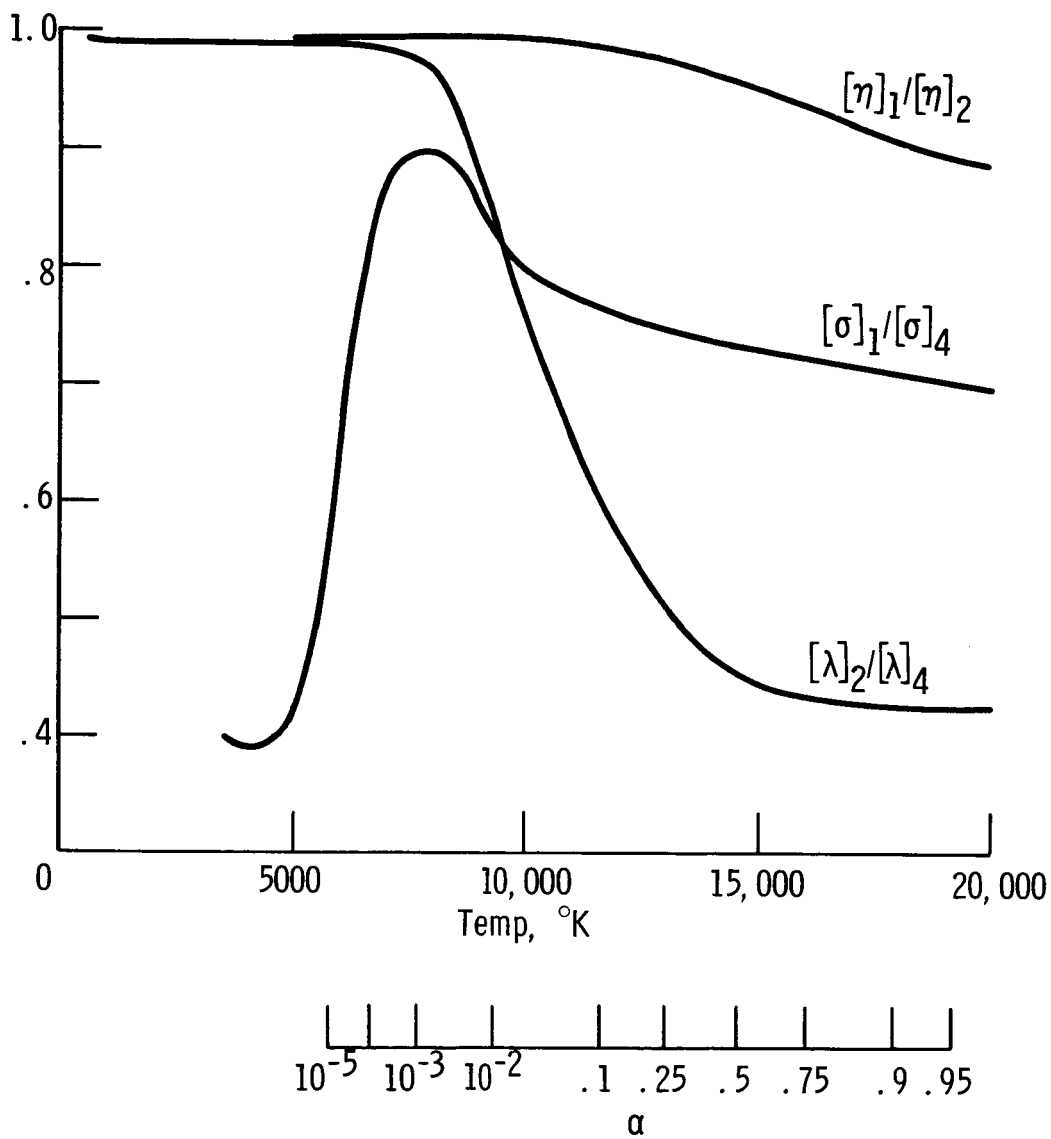


Fig. 10. - Comparison of lowest Chapman Enskog approximations with higher approximations. (Argon, 1 atmosphere).

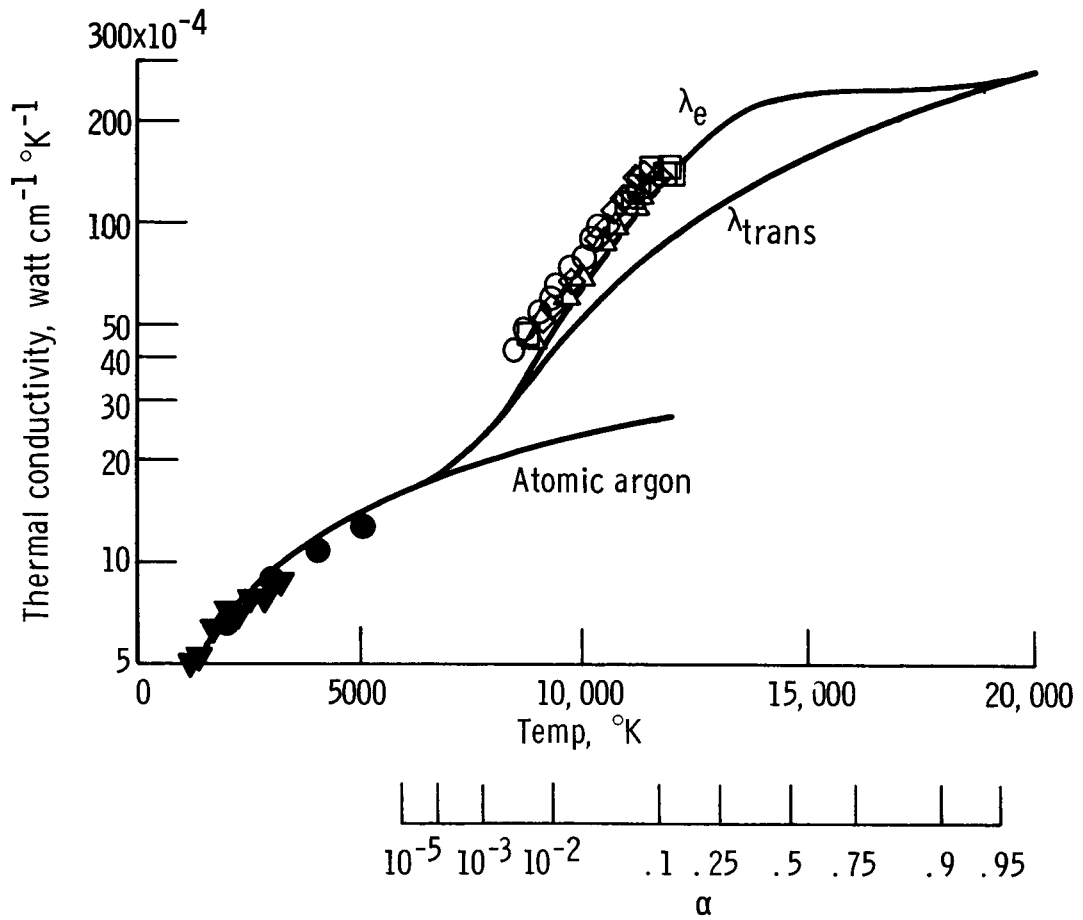


Fig. 11. - Thermal conductivity of partially ionized argon, (1 atm).

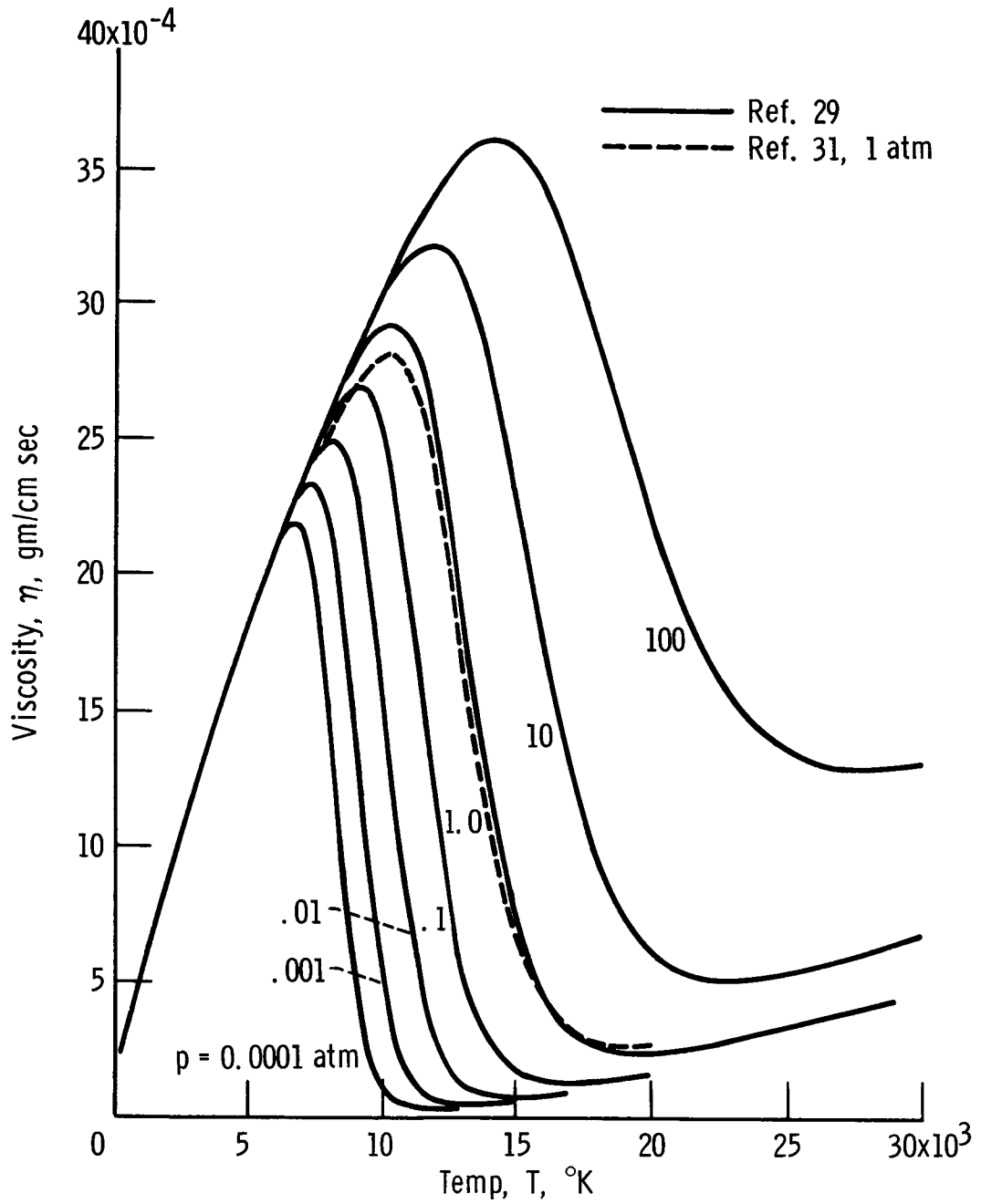


Fig. 12. - Viscosity of partially ionized argon as a function of temperature.